The transcription factor RIP140 regulates interferon γ signaling in breast cancer

S. Jalaguier[1]*, A. Kuehn[1], C. Petitpas[1], A. Dulom[1], R. Jacquemont[1], C. Assi[1], S. Sixou[2], U. Jeschke[3], J. Colinge[1*] and V. Cavaillès[1,4]

[1]IRCM, Institut de Recherche en Cancérologie de Montpellier, Montpellier, F-34298, France; INSERM, U1194, Montpellier, F-34298, France; Université de Montpellier, Montpellier, F-34090, France; Institut régional du Cancer de Montpellier, Montpellier, F-34298, France.

[2]Faculté des Sciences Pharmaceutiques, Université Toulouse III—Paul Sabatier, F-31062 Toulouse, France.

[3]Department of Obstetrics and Gynecology, University Hospital Augsburg, Stenglinstrasse 2, 86156 Augsburg, Germany.

[4]CNRS, Montpellier, F-34298, France.

Corresponding authors : Stéphan Jalaguier, IRCM, Institut de Recherche en Cancérologie de Montpellier, INSERM, U1194, 208 rue des Apothicaires, 34298 Montpellier cedex 5, France; Tel: (33)411283174; E-mail: stephan.jalaguier@inserm.fr, Jacques Colinge, IRCM, Institut de Recherche en Cancérologie de Montpellier, INSERM, U1194, 208 rue des Apothicaires, 34298 Montpellier cedex 5, France; Tel: (33)411283118; E-mail: jacques.colinge@umontpellier.fr

Running title: RIP140 and IFNγ signaling in breast cancer

Keywords: RIP140/NRIP1, interferon-γ, GBP1, gene expression, cell proliferation, breast cancer.

Abbreviations: BC, breast cancer; GBP1, guanylate binding protein1; NRIP1, nuclear receptor interacting protein 1; RIP140, receptor-interacting protein of 140 kDa; SP100, SP100 nuclear antigen; VDR, vitamin D receptor.

ABSTRACT

RIP140 (receptor interacting protein of 140 kDa) is an important player in breast cancer (BC) by regulating key cellular pathways such as nuclear hormone receptors signaling. In order to identify additional genes specifically regulated by RIP140 in BC, we performed an RNA sequencing after silencing its expression in MCF-7 cells. Many genes were isolated including the vitamin D receptor, whose regulation was validated by qPCR. Most importantly, interferon γ (IFNγ) signaling was substantially controled by RIP140. We identified GBP1 (guanylate binding protein 1), a prime IFNγ effector, as robustly stimulated by RIP140 through an ISRE motif, while IFNγ-dependent expression of GBP1 was repressed by the transcriptional coregulator. Furthermore, we showed that RIP140 modulated IFNγ-dependent repression of BC cell proliferation. Finally, reanalysis of transcriptomic data revealed that IFNγ expression was associated with good prognosis only for BC patients exhibiting tumors expressing low levels of RIP140, thus confirming its effect on the anti-tumor activity of IFNγ provided by our experimental data. Altogether, this study identifies RIP140 as a major regulator of IFNγ signaling in breast tumorigenesis.

174 words

1. Introduction

Breast cancer (BC) is the most common tumor for women in the world. In 2020, according to the World Health Organization, over two million women were diagnosed with a breast cancer and more than 600 000 died of that pathology. A diversity of signaling pathways, which strongly cross-talk, cause survival and proliferation of BC cells. One of the most important, from a clinical point of view, involves estrogen receptor α (ERα) which drives around 70 % of BC [1].

Other pathways are implicated such as the mitogen-activated protein kinase (MAPK) [2], the Notch [3], the phosphoinositide-3-kinase-protein kinase B (PI3K/AKT) [4] or the Janus kinase/signal transducers and activator of transcription (JAK/STAT) pathways [5]. Interferon-γ/STAT1 (IFNγ/STAT1) signaling can also induce tumor cell apoptosis and results in repression of BC cell growth [6]. In addition to prompt apoptosis and senescence, IFNγ can shift tumors to a dormant state [7]. It must also be underlined that this pathway is believed to be critical for the success of immune therapy [8]. However, in the tumor microenvironment, IFNγ can manage both pro-carcinogenic as well as antitumor immunity [8].

RIP140 (receptor interacting protein of 140kDa) [9], also known as NRIP1 (nuclear receptor interacting protein 1), was shown to play an active role in many physiological or pathological processes. For instance, mice lacking the *Rip140* gene displayed a female infertility, a reduced body fat content and severe cognitive defects [10]. RIP140 regulates mammary gland development by directly regulating the expression of the progesterone receptor, amphiregulin and signal transducer and activator of transcription 5a [11]. In BC, we showed that a decreased expression of RIP140 activity was associated with the bad prognosis basal-like tumors [12] while an increase in RIP140 mRNA was observed in overall breast tumors [13]. Very recently, our team evidenced that RIP140 could repress proliferation of BC cells by targeting glycolysis (more precisely GLUT3 expression) [14] and the phosphate pentose pathway through inhibition of glucose 6-phosphate dehydrogenase [15].

For a better understanding of RIP140 action in BC, we performed an RNA sequencing analysis of MCF7 cells presenting a downregulation of *NRIP1*. A large number of target genes were upregulated by RIP140, as expected from its role as a transcriptional repressor, but others were significantly down-regulated including for instance the vitamin D receptor. We evidenced the interferon signaling as a target of RIP140. By focusing on GBP1 as a main IFNγ-induced gene, we demonstrated that

its IFNγ-dependent expression in three BC cell lines (MCF7, T47D and MDA-MB-231) was regulated by RIP140. This regulation occurs at the transcriptional level through an IFN-response element. Finally, we showed that RIP140 affected the regulation of BC cell proliferation by IFNγ and reanalysis of transcriptomics data from BC patient samples validated the impact of RIP140 on the prognosis value of the *IFNG* gene expression. Altogether, our data suggest that the IFNγ/GBP1 signaling may partly drive the antiproliferative effect of RIP140 observed in BC cells

2. Materials and methods

2.1. Materials

Estradiol and Interferon γ were purchased from Sigma-Aldrich ®.

2.2. Plasmids

pEFcmyc-RIP140 was previously described [16]. Pro3757-hGBP1, pro237-hGBP1 and ΔISRE-hGBP1 were kindly provided by Dr Elisabeth Naschberger[17]. pISRE-F-luc was a generous gift from Dr Konstantin Maria Johannes Sparrer[18].

2.3. RNA-seq data generation and processing

RNA extracts were submitted to Illumina sequencing following a single end 1x75bp protocol. Read sequences were cut to eliminate the first 13 nucleotides due to compositional bias. Low quality ends were further trimmed with sickle. The resulting shortened reads were aligned against the human genome (hg38) with the TopHat 2.1.0 algorithm. Gene expression data (read counts) were obtained applying HTSeq-count to extract the number of reads aligned over each protein-coding gene. Read counts were compiled in a gene expression matrix. Genes that did not reach a minimum read count of 5 in at least 4 samples were considered not expressed and thus discarded. The remaining expression matrix was normalized with edgeR [19] TMM method. We then constructed a statistical model of the whole data set using edgeR robust negative binomial generalized linear model with a design matrix linking the two replicates of each condition. Pairwise gene selections, e.g. siRIP140 against siCtl unstimulated (ethanol), were subsequently obtained from the globally calibrated model. In every case, we imposed a p-value<0.01, a minimum $\log_2$-fold-change of 0.5 in absolute value (1.4 in the linear scale), and an average minimum read count over all the samples of the two tested conditions of 20.

2.4. Pathway analysis

Gene set enrichment analysis was conducted with R BioConductor FGSEA library [20] using GO Biological Process terms and Reactome pathways as gene sets. FGSEA was run with 1,000,000 permutations and we imposed minimum and maximum gene set sizes of 15 and 250 respectively.

2.5. Cell culture and transfections

MELN cells were cultured in phenol red-free DMEM-F12 (Invitrogen) containing 5% dextran-charcoal treated FCS (Invitrogen), MCF7 (RRID:CVCL_0031) and MDA-MB-231 (RRID:CVCL_0062) in DMEM-F12 (Invitrogen) and T47D (RRID:CVCL_0553) in RPMI (Invitrogen) supplemented with 10% fetal calf serum (FCS) and antibiotics (Gibco). All cell lines were authenticated by short tandem repeat profiling and tested for mycoplasma contamination. When needed, plasmids or siRNAs were transfected using either JetPEI or INTERFERin (Polyplus), respectively. When indicated, cells were treated with 100 nM E2 or 10 µg/ml IFNγ and then harvested 24 hours later. The list and sequences of the siRNAs used in this study are indicated in Supplementary table 1.

2.6. mRNA quantification

RNA was isolated using the Zymo Research kit (Zymo research) and reverse transcription (RT)-qPCR assays were done using qScript (VWR) according to the manufacturer's protocol. Transcripts were quantified using SensiFAST SYBR (BioLine) on a LC480 instrument. The nucleotide sequences of the primers used for real time PCR are indicated in Supplementary Table 1.

2.7. Immunoblotting assays

Western blot analyses were performed as previously described [13] using anti-VDR (Ozyme), anti-GBP1 (Origene) or anti-actin (Sigma) antibodies.

2.8. Luciferase assays

MCF7, MDA-MB-231 and T47D cells were plated in 96-well plates 24 hours prior to transfection with either JetPEI or INTERFERin according to the manufacturer's protocol. Firefly luciferase data were normalized to renilla luciferase activity and

expressed as relative luciferase activities.

2.9. Cell proliferation assay

MCF7, MDA-MB-231 and T47D cells were seeded at a density of 2000 cells per well. At the indicated time, 0.5 mg/ml 3-(4,5-dimethylthiazol-2-yl)-2,5-diphenyltetrazolium bromide (MTT) (Sigma-Aldrich, St Louis, MO, USA) was added to selected wells and cells were incubated at 37°C for 4h. Formazan crystals were solubilized in DMSO and absorbance read at 560 nm on a spectrophotometer. Results were normalized to the cell density at day 1.

2.10. Survival analysis

Using the KM-plot Private Edition (http://kmplot.com) [21], RNA sequencing data from the Cancer Genome Atlas (TCGA) were analyzed using Cox proportional hazards regression, as previously described [22]. The Kaplan-Meier method was used to estimate overall survival calculated from diagnosis to death. Patients lost to follow-up were censored at the time of last contact.

2.11. Statistical analysis

All experiments were conducted independently at least three times. Results were expressed as the mean ± standard deviation (S.D.). Comparisons of two independent groups were performed using the Mann-Whitney U test. A probability level (*p* value) of 0.05 was chosen for statistical significance. Statistical analyses were performed using StatEL (AdScience).

3. Results

3.1. Identification and validation of RIP140 target genes in BC cells

In order to get a comprehensive survey of RIP140 target genes in BC cells, we performed an RNA sequencing using MELN cells derived from MCF7 BC cells stably expressing luciferase under the control of estrogen responsive elements [23]. We first validated RIP140 silencing using small interfering RNA (siRIP140) transfection by showing that these cells expectedly displayed a reduced expression of RIP140 mRNA (almost 80% decrease as shown in Figure 1A) as well as a 2-fold increased estradiol-dependent regulation of luciferase expression (Figure 1B).

An RNA sequencing analysis of these BC cells transfected or not with siRIP140 was then performed in the absence of estradiol. On Table 1 are showed the genes ranked according to the best p value and a negative (Top panel) or positive (Bottom panel) amplitude fold. Interestingly, downregulation of RIP140 expression does not induce drastic variations in target genes expression, a phenomenon we long experienced.
The RNA sequencing results were then validated by RT-qPCR assays. As shown in Figure 1C, we validated several genes down-regulated under siRIP140 transfection, including the vitamin D receptor (*VDR*), acyl-CoA binding domain containing 5 (*ACBD5*) and macrophage erythroblast attacher (*MAEA*). Ectopic expression of RIP140 in MCF7 cells, induced the opposite effect, *i.e.* an up-regulation of the three above mentioned genes (Figure 1D). Similar results were obtained in the T47D luminal BC cell line, and for VDR, the regulation by RIP140 was validated at the protein level (Data not shown). Altogether, these data validated the robustness of our RNA sequencing analysis.

3.2. Interferon γ signaling is a target of RIP140

The gene set enrichment analysis (GSEA) of our sequencing data allowed us to identify a series of over-represented genes, significantly enriched or depleted, associated to a phenotype. Accordingly, IFNγ signaling, a major pathway in breast carcinogenesis appeared on top of the list (Table 2). More precisely, five genes belonging to this pathway were identified as being regulated by RIP140, guanylate binding protein 1 (GBP1), SP100 nuclear antigen (SP100), major histocompatibility complex, class I, G (HLA-G), major histocompatibility complex, class II, DP alpha 1 (HLA-DPA1) and interferon beta 1 (IFNB) (data not shown). GBP1 being described as one of the most significantly induced proteins in cells exposed to IFNγ [24], and shown to play a major role in BC [25], this prompted us to further investigate the regulation of this gene by RIP140.

3.3. RIP140 increases GBP1 expression in BC cells

When transfected with siRIP140, MCF7 cells as well as T47D and MDA-MB-231 cells displayed a significant decrease (between 20 and 40 %) in GBP1 mRNA expression (Figure 2A), confirming the data obtained with MELN cells (Supplementary Figure 1A, left panel). Transfection of an additional siRIP140, allowed us to validate these observation (Supplementary Figure 1A, right panel). Using pro-GBP-1, a reporter

construct with the GBP1 promoter driving the luciferase gene [17], we demonstrated that silencing RIP140 activity in MCF7, T47D and MDA-MB-231 cells reduced GBP1 promoter activity (Figure 2B). Conversely, when transfecting increasing doses of RIP140 expression plasmid, we observed that activity augmented both in MCF7 (Figure 2C) and T47D (Figure 2D) cells, indicating a transcriptional regulation of GBP1 expression by RIP140. In parallel, we also investigated the regulation of Sp100. As exhibited in Supplementary Figure 1B, a transfection of siRIP140 or siRIP140#1 also decreased Sp100 mRNA expression in MELN, MCF7 and T47D cells, while ectopic expression of RIP140 significantly augmented it (Supplementary Figure 1C). From these two examples, also consolidated by other IFNγ-regulated genes (such as *HLA-G*, *HLA-DPA1* or *IFNB1*) (data not shown), we concluded that, in various BC cells, RIP140 increased expression of IFNγ signaling pathway actors.

3.4. RIP140 regulates GBP1 expression through an ISRE binding site

In order to unveil RIP140 mechanism of action on the regulation of GBP1 expression, we used a shorter version of the GBP1 promoter, *i.e.* pro237-GBP1 (Figure 3A), together with a ΔISRE mutated form, where the interferon specific response element (ISRE) is mutated [17] (Figure 3B). As shown in Figure 3C, transfection of siRIP140 induced a very similar decrease of pro237-GBP1 activity in MCF7, T47D and MDA-MB-231 cells as the one observed with pro-GBP-1 (Figure 2B), indicating the two constructs behaved similarly. The same result was also obtained when using siRIP140#1 (Supplementary Figure 1D, left panel). Interestingly, transfection of siRIP140 (Figure 5D) or siRIP140#1 (Supplementary Figure 1D, right panel) induced no change in ΔISRE activity revealing the importance of the response element for RIP140-dependent regulation of GBP1 promoter. Furthermore, we used a reporter plasmid consisting of five repeated ISRE sequences upstream the luciferase gene (Figure 3E, left panel). As shown in Figure 3F (right panel), both MCF7 and T47D transfected with the vector and siRIP140 displayed a significant reduction of luciferase activity. These results indicate a need for a valid ISRE to mediate RIP140 transcriptional response on the GBP1 promoter.

3.5. RIP140 represses IFNγ-induced GBP1 expression

Upon treatment of MCF7, T47D and MDA-MB-231 cells with IFNγ (Figure 4A), expression of GBP1 mRNA was robustly stimulated (especially in T47D cells), further

confirming GBP1 as a major target of IFNγ. A milder induction but still significant was also observed when the same cell lines were transfected with the pro-GBP-1 plasmid and treated with the same doses of IFNγ (data not shown).

We next wondered whether RIP140 could affect IFNγ-induced GBP1 expression. After depletion of RIP140 mRNA and treatment with increasing doses of IFNγ, we observed that the difference in GBP1 expression between siRIP140 and siCtl augmented with the dose of IFNγ in both MCF7 (Figure 4B) and T47D cells (Supplementary Figure 2B). At the protein level, while expression of RIP140 in MCF7 cells was low in basal conditions (transfection with siCtl and DMSO treatment) (Figure 4C, left panel), a decrease was observed under siRIP140 transfection (see the right panel for quantification). Remarkably, IFNγ induced a strong GBP1 expression, amplified when lowering RIP140 expression, confirming results obtained with mRNA. Likewise, IFNγ induction of GBP1 expression was stronger when depleting RIP140 mRNA in all three cell lines, with a stronger effect in T47D (Figure 4D). We also observed a significantly stronger IFNγ-induced activity of pro-GBP-1 under transfection of siRIP140 in MCF7, T47D and MDA-MB-231 (Figure 4E). Conversely, when ectopically expressing increasing doses of RIP140, IFNγ-induced activity of pro-GBP-1 decreased both in MCF7 (Figure 4F) and T47D (Figure 4G) cells. In MCF7, T47D or MDA-MB231 cells transfected with RIP140, ΔISRE plasmid could no longer be stimulated by IFNγ (Supplementary Figure 2C), further demonstrating the role of the ISRE element in mediating both RIP140 and IFNγ signaling.

In parallel, focusing on Sp100 expression we showed that IFNγ significantly stimulated its mRNA expression in MCF7, T47D and MDA-MB-231 cells (Supplementary Figure 2D). We also demonstrated that IFNγ induction of Sp100 expression was stronger when transfecting siRIP140 (MCF7 and T47D cells, Supplementary Figure 2E, left panel) or siRIP140#1 (MCF7 and MDA-MB-231, Supplementary Figure 2E, right panel). This series of experiments demonstrated that RIP140 prevents a full stimulatory effect of IFNγ on the expression of these two target genes.

3.6. RIP140 regulates IFNγ-driven BC cell proliferation

Based on the effect of RIP140 on IFNγ-target genes, we then wondered whether RIP140 could modulate IFNγ-dependent BC cell proliferation. Using MTT assays, we

first confirmed that IFNγ inhibited the growth of MCF7 and MDA-MB-231 cells (Figure 5A, left and right panels), with a more marked effect on the latter ones. Using the same means, the two BC cell lines transfected with siRIP140 exhibited a gain in cell proliferation (Figure 5B), validating that RIP140 displays anti-proliferative properties in BC cells. When down-regulating RIP140 expression, we observed that IFNγ acted as a stronger repressor of either MCF7 (Figure 5C, left panel) or MDA-MB-231 (Figure 5C, right panel) cell proliferation, indicating that RIP140 prevents the cytokine to fully exert its antiproliferative effect.

3.7. RIP140 expression determine the prognosis value of *IFNG* gene in BC

The experimental data shown in Fig 5C strongly suggested that high levels of RIP140 expression should inhibit the antiproliferative activity of IFNγ. We therefore hypothesized that, in breast cancers, low RIP140 levels could be a marker of such an IFNγ anti-tumor activity and consequently, that *IFNG* gene expression might be associated with an increased overall survival for patients with tumor expressing a reduced level of RIP140. Using Cox proportional hazard regression [32], we analyzed RNAseq data obtained from 1068 breast tumor samples from the TCGA dataset as described previously [33] (Figure 6). We first checked the prognostic values of the expression of each gene by analyzing patient overall survival at 60 months. High *IFNG* expression was correlated with good prognosis (HR 0.59, p=0.0011) (Figure 6A). Then we used the median as a cutoff value for classification of patients into two groups of tumors with low and high RIP140 expression, respectively. Using Kaplan-Meier plots, we investigated whether *IFNG* expression correlated with OS at 60 months within both groups using the same cutoff values. Interestingly, IFNG expression was significantly associated with increased overall survival in low RIP140 expression group (p=0.0017) but not in high RIP140 expression group (p=0.47) (Figure 6B).

4. Discussion

In this study, we performed a transcriptomic analysis after silencing RIP140 in MCF7 cells. We confirmed by means of qPCR, RIP140-dependent regulation of some genes, including VDR. Analysis of the sequencing data allowed us to identify IFNγ targets as being substantially modulated by RIP140. Accordingly, we identified GBP1 as a robustly RIP140-regulated gene and we described how both RIP140 and GBP1

could drive IFNγ-driven inhibition of breast cancer cell proliferation.

GBPs are a family of proteins described as IFN-inducible GTPases which can induce antimicrobial immunity and cell death [26]. GBP1 was also associated to a bad prognosis for triple negative breast cancers [25]. In this latter study, it must be underlined that in proliferation assays, GBP1 was shown oncogenic in MDA-MB-231 cell, whereas we described it with an anti-proliferative activity. Moreover, GBP1 expression is very heterogeneous depending on the type of cancer [27]. It is oncogenic in prostate cancer [28], its expression correlates with worse survival in lung cancer [29,30], it is associated to treatment resistance in ovarian cancer [31] and overexpression of GBP1 is correlated to a poor prognosis and promotes tumor growth in glioblastoma [32]. Conversely, GBP1 was described as a tumor suppressor in colon cancer [33]. These observations remind of RIP140 which has a protective role in colon [34] or triple negative breast cancer [13,35] whereas a high expression is associated with stomach cancer [36] as well as a shorter overall survival of cervical cancer patients [37]. GBP1 and RIP140 are a good illustration of tissue specificity of gene activity.

In this study, we described cross-talks between RIP140 and IFNγ on common transcriptional targets, mainly GBP1 and Sp100. However, we can also highlight other examples, especially E2F1 transcription factor whose expression is down-regulated by IFNγ in T47D cells [38] while RIP140 represses E2F1 activity [39]. A similar cross-talk involves the androgen receptor (AR) since IFNγ is described to increase the receptor expression in prostate [40] while we describe a repressive activity of RIP140 on agonist-liganded AR in prostate cancer cells [41]. We also evidenced that RIP140 was able to repress estradiol-induced AP1 activity [42] which was also described to induce IFNγ expression [43].

IFNγ is described to have anti-tumorigenic effects, noticeably by promoting apoptosis through induction of caspases expression (caspase 8 and caspase 9) [44]. Interestingly, our RNA sequencing data together with qPCR assays evidenced a positive effect of RIP140 on the expression of the two caspases (data not shown). Alongside, IFNγ is able to repress metastasis progression though induction of fibronectin 1 (FN1) expression [45]. Again, we also found that RIP140 was able to induce FN1 expression. Together with our cell proliferation assay, the effect of RIP140 on apoptosis and metastasis markers expression argues for a protective role of RIP140 on tumor development. By sharp contrast, low doses of IFNγ may have

pro-tumorigenic effects by inducing tumor stemness through induction of ICAM1 expression [46]. Like IFNγ, RIP140 can also induce ICAM1 (data not shown), therefore participating to a potential pro-tumorigenic effect. Interestingly, RIP140 has the same action as IFNγ on many genes, including the yin and yang effect on carcinogenesis.

IFNγ also participates to cancer evasion by promoting carcinogenesis and angiogenesis. It is well characterized for papillary thyroid cancer cells where IFNγ induces epithelial-mesenchymal transition (EMT) and increases migration and invasion of the cancer cells [47]. Even though RIP140 was not shown to promote EMT, we demonstrated that its cytoplasmic expression in breast cancer cells correlates with the expression of N-cadherin, a marker of EMT [48]. Accordingly, together with IFNγ, RIP140 could be envisaged to participate to cancer evasion.

Finally, it has long been accepted that IFNγ plays a central role in host antitumor immunity[49]. Indeed, tumor-infiltrating lymphocytes, essential for cancer immune surveillance are the main source of IFNγ in tumors [49]. Non-small cell lung cancer and melanoma patients treated with a PD-1 inhibitor display an increase in IFNγ protein expression accompanied with a longer progression-free survival [50], which could indicate the cytokine as a biomarker for prediction of response to immune checkpoint blockade. Since we describe RIP140 as a repressor of IFNγ-induced target genes, its own expression could also be hypothesized as a biomarker of the checkpoint blockade.

In conclusion, identifying IFNγ as a new target of RIP140, reinforces the major role of this transcription factor in carcinogenesis, not only within the tumor but also potentially in the tumor microenvironment.

Author contributions

SJ participated to conceptualization, generation of data and writing, AK, CP, AD, RJ and CA generated data, SS and UJ contributed to analysis of data and JC and VC participated to conceptualization, writing and funding acquisition.

Acknowledgements

We would like to thank Dr Elisabeth Naschberger for the kind gift of pro3757-GBP1, pro237-GBP1 and ΔISRE plasmids as well as Dr Konstantin Maria Johannes Sparrer for the generous gift of pISRE-F-luc.

We are grateful to Dr Catherine Teyssier for the critical reading of the manuscript.

We gratefully acknowledge the financial support of Groupement des Entreprises Françaises dans la Lutte contre le Cancer (GEFLUC).

Conflict of interest

No conflict of interest to declare

References

1 Siersbæk R, Kumar S, Carroll JS. Signaling pathways and steroid receptors modulating estrogen receptor α function in breast cancer. *Genes Dev*. 2018;**32**(17–18):1141–1154.

2 Sivaraman VS, Wang H, Nuovo GJ, Malbon CC. Hyperexpression of mitogen-activated protein kinase in human breast cancer. *J Clin Invest*. 1997;**99**(7):1478–1483.

3 Acar A, Simões BM, Clarke RB, Brennan K. A Role for Notch Signalling in Breast Cancer and Endocrine Resistance. *Stem Cells Int*. 2016;**2016**:2498764.

4 Luo J, Manning BD, Cantley LC. Targeting the PI3K-Akt pathway in human cancer: rationale and promise. *Cancer Cell*. 2003;**4**(4):257–262.

5 Alvarez JV, Febbo PG, Ramaswamy S, Loda M, Richardson A, Frank DA. Identification of a genetic signature of activated signal transducer and activator of transcription 3 in human tumors. *Cancer Res*. 2005;**65**(12):5054–5062.

6 Gooch JL, Herrera RE, Yee D. The role of p21 in interferon gamma-mediated growth inhibition of human breast cancer cells. *Cell Growth Differ Mol Biol J Am Assoc Cancer Res*. 2000;**11**(6):335–342.

7 Müller-Hermelink N, Braumüller H, Pichler B, Wieder T, Mailhammer R, Schaak K, et al. TNFR1 signaling and IFN-gamma signaling determine whether T cells induce tumor dormancy or promote multistage carcinogenesis. *Cancer Cell*. 2008;**13**(6):507–518.

8 Jorgovanovic D, Song M, Wang L, Zhang Y. Roles of IFN-γ in tumor progression and regression: a review. *Biomark Res*. 2020;**8**:49.

9 Cavaillès V, Dauvois S, L'Horset F, Lopez G, Hoare S, Kushner PJ, et al. Nuclear factor RIP140 modulates transcriptional activation by the estrogen receptor. *EMBO J*. 1995;**14**(15):3741–3751.

10 Nautiyal J. Transcriptional coregulator RIP140: an essential regulator of physiology. *J Mol Endocrinol*. 2017;**58**(3):R147–R158.

11 Nautiyal J, Steel JH, Mane MR, Oduwole O, Poliandri A, Alexi X, et al. The transcriptional co-factor RIP140 regulates mammary gland development by promoting the generation of key mitogenic signals. *Dev Camb Engl*. 2013;**140**(5):1079–1089.

12 Docquier A, Harmand P-O, Fritsch S, Chanrion M, Darbon J-M, Cavaillès V. The transcriptional coregulator RIP140 represses E2F1 activity and discriminates breast cancer subtypes. *Clin Cancer Res Off J Am Assoc Cancer Res*. 2010;**16**(11):2959–2970.

13 Jalaguier S, Teyssier C, Nait Achour T, Lucas A, Bonnet S, Rodriguez C, et al. Complex regulation of LCoR signaling in breast cancer cells. *Oncogene*. 2017;**36**(33):4790–4801.

14 Jacquier V, Gitenay D, Fritsch S, Bonnet S, Győrffy B, Jalaguier S, et al. RIP140 inhibits glycolysis-dependent proliferation of breast cancer cells by regulating GLUT3 expression through transcriptional crosstalk between hypoxia induced factor and p53. *Cell Mol Life Sci CMLS*. 2022;**79**(5):270.

15 Jacquier V, Gitenay D, Cavaillès V, Teyssier C. The Transcription Coregulator RIP140 Inhibits Cancer Cell Proliferation by Targeting the Pentose Phosphate Pathway. *Int J Mol Sci*. 2022;**23**(13):7419.

16 Carascossa S, Gobinet J, Georget V, Lucas A, Badia E, Castet A, et al. Receptor-interacting protein 140 is a repressor of the androgen receptor activity. *Mol Endocrinol Baltim Md*. 2006;**20**(7):1506–1518.

17 Naschberger E, Werner T, Vicente AB, Guenzi E, Töpolt K, Leubert R, et al. Nuclear factor-kappaB motif and interferon-alpha-stimulated response element co-operate in the activation of guanylate-binding protein-1 expression by inflammatory cytokines in endothelial cells. *Biochem J*. 2004;**379**(Pt 2):409–420.

18 Hirschenberger M, Hayn M, Laliberté A, Koepke L, Kirchhoff F, Sparrer KMJ. Luciferase reporter assays to monitor interferon signaling modulation by SARS-CoV-2 proteins. *STAR Protoc*. 2021;**2**(4):100781.

19 Ritchie ME, Phipson B, Wu D, Hu Y, Law CW, Shi W, et al. limma powers differential expression analyses for RNA-sequencing and microarray studies. *Nucleic Acids Res*. 2015;**43**(7):e47.

20 Sergushichev AA. An algorithm for fast preranked gene set enrichment analysis using cumulative statistic calculation. *bioRxiv*. 2016;060012.

21 Györffy B, Lanczky A, Eklund AC, Denkert C, Budczies J, Li Q, et al. An online survival analysis tool to rapidly assess the effect of 22,277 genes on breast cancer prognosis using microarray data of 1,809 patients. *Breast Cancer Res Treat*. 2010;**123**(3):725–731.

22 Nagy Á, Munkácsy G, Győrffy B. Pancancer survival analysis of cancer hallmark genes. *Sci Rep*. 2021;**11**(1):6047.

23 Balaguer P, Boussioux AM, Demirpence E, Nicolas JC. Reporter cell lines are useful tools for monitoring biological activity of nuclear receptor ligands. *Lumin J Biol Chem Lumin*. 2001;**16**(2):153–158.

24 Lubeseder-Martellato C, Guenzi E, Jörg A, Töpolt K, Naschberger E, Kremmer E, et al. Guanylate-binding protein-1 expression is selectively induced by inflammatory cytokines and is an activation marker of endothelial cells during inflammatory diseases. *Am J Pathol*. 2002;**161**(5):1749–1759.

25 Quintero M, Adamoski D, Reis LMD, Ascenção CFR, Oliveira KRS de, Gonçalves K de A, et al. Guanylate-binding protein-1 is a potential new therapeutic target for triple-negative breast cancer. *BMC Cancer*. 2017;**17**(1):727.

26 Honkala AT, Tailor D, Malhotra SV. Guanylate-Binding Protein 1: An Emerging Target in Inflammation and Cancer. *Front Immunol*. 2019;**10**:3139.

27 Zhao Y, Wu J, Li L, Zhang H, Zhang H, Li J, et al. Guanylate-Binding Protein 1 as a Potential Predictor of Immunotherapy: A Pan-Cancer Analysis. *Front Genet*. 2022;**13**:820135.

28 Zhao J, Li X, Liu L, Cao J, Goscinski MA, Fan H, et al. Oncogenic Role of Guanylate Binding Protein 1 in Human Prostate Cancer. *Front Oncol*. 2019;**9**:1494.

29 Wan Q, Qu J, Li L, Gao F. Guanylate-binding protein 1 correlates with advanced tumor features, and serves as a prognostic biomarker for worse survival in lung adenocarcinoma patients. *J Clin Lab Anal*. 2021;**35**(2):e23610.

30 Meng Y, Wang W, Chen M, Chen K, Xia X, Zhou S, et al. GBP1 Facilitates Indoleamine 2,3-Dioxygenase Extracellular Secretion to Promote the Malignant Progression of Lung Cancer. *Front Immunol*. 2020;**11**:622467.

31 Duan Z, Foster R, Brakora KA, Yusuf RZ, Seiden MV. GBP1 overexpression is associated with a paclitaxel resistance phenotype. *Cancer Chemother Pharmacol*. 2006;**57**(1):25–33.

32 Ji X, Zhu H, Dai X, Xi Y, Sheng Y, Gao C, et al. Overexpression of GBP1 predicts poor prognosis and promotes tumor growth in human glioblastoma multiforme. *Cancer Biomark Sect Dis Markers*. 2019;**25**(3):275–290.

33 Britzen-Laurent N, Lipnik K, Ocker M, Naschberger E, Schellerer VS, Croner RS, et al. GBP-1 acts as a tumor suppressor in colorectal cancer cells. *Carcinogenesis*. 2013;**34**(1):153–162.

34 Lapierre M, Bonnet S, Bascoul-Mollevi C, Ait-Arsa I, Jalaguier S, Del Rio M, et al. RIP140 increases APC expression and controls intestinal homeostasis and tumorigenesis. *J Clin Invest*. 2014;**124**(5):1899–1913.

35 Yu X-H, Xue X, Zhu X, Li X. Downregulation of RIP140 in triple-negative breast cancer inhibits the growth and proliferation of cancer cells. *Oncol Lett*. 2018;**15**(6):8784–8788.

36 Triki M, Ben Ayed-Guerfali D, Saguem I, Charfi S, Ayedi L, Sellami-Boudawara T, et al. RIP140 and LCoR expression in gastrointestinal cancers. *Oncotarget*. 2017;**8**(67):111161–111175.

37 Vattai A, Cavailles V, Sixou S, Beyer S, Kuhn C, Peryanova M, et al. Investigation of RIP140 and LCoR as independent markers for poor prognosis in cervical cancer. *Oncotarget*. 2017;**8**(62):105356–105371.

38 Reimer D, Sadr S, Wiedemair A, Concin N, Hofstetter G, Marth C, et al. Heterogeneous cross-talk of E2F family members is crucially involved in growth modulatory effects of interferon-gamma and EGF. *Cancer Biol Ther*. 2006;**5**(7):771–776.

39 Docquier A, Harmand P-O, Fritsch S, Chanrion M, Darbon J-M, Cavaillès V. The transcriptional coregulator RIP140 represses E2F1 activity and discriminates breast cancer subtypes. *Clin Cancer Res Off J Am Assoc Cancer Res*. 2010;**16**(11):2959–2970.

40 Basrawala Z, Alimirah F, Xin H, Mohideen N, Campbell SC, Flanigan RC, et al. Androgen receptor levels are increased by interferons in human prostate stromal and epithelial cells. *Oncogene*. 2006;**25**(19):2812–2817.

41 Carascossa S, Gobinet J, Georget V, Lucas A, Badia E, Castet A, et al. Receptor-interacting protein 140 is a repressor of the androgen receptor activity. *Mol Endocrinol Baltim Md*. 2006;**20**(7):1506–1518.

42 Teyssier C, Belguise K, Galtier F, Cavailles V, Chalbos D. Receptor-interacting protein 140 binds c-Jun and inhibits estradiol-induced activator protein-1 activity by reversing glucocorticoid receptor-interacting protein 1 effect. *Mol Endocrinol Baltim Md*. 2003;**17**(2):287–299.

43 Ye J, Cippitelli M, Dorman L, Ortaldo JR, Young HA. The nuclear factor YY1 suppresses the human gamma interferon promoter through two mechanisms: inhibition of AP1 binding and activation of a silencer element. *Mol Cell Biol*. 1996;**16**(9):4744–4753.

44 Kundu M, Roy A, Pahan K. Selective neutralization of IL-12 p40 monomer induces death in prostate cancer cells via IL-12-IFN-γ. *Proc Natl Acad Sci U S A*. 2017;**114**(43):11482–11487.

45 Glasner A, Levi A, Enk J, Isaacson B, Viukov S, Orlanski S, et al. NKp46 Receptor-Mediated Interferon-γ Production by Natural Killer Cells Increases Fibronectin 1 to Alter Tumor Architecture and Control Metastasis. *Immunity*. 2018;**48**(1):107-119.e4.

46 Song M, Ping Y, Zhang K, Yang L, Li F, Zhang C, et al. Low-Dose IFNγ Induces Tumor Cell Stemness in Tumor Microenvironment of Non-Small Cell Lung Cancer. *Cancer Res*. 2019;**79**(14):3737–3748.

47 Lv N, Gao Y, Guan H, Wu D, Ding S, Teng W, et al. Inflammatory mediators, tumor necrosis factor-α and interferon-γ, induce EMT in human PTC cell lines. *Oncol Lett*. 2015;**10**(4):2591–2597.

48 Sixou S, Müller K, Jalaguier S, Kuhn C, Harbeck N, Mayr D, et al. Importance of RIP140 and LCoR Sub-Cellular Localization for Their Association With Breast Cancer Aggressiveness and Patient Survival. *Transl Oncol*. 2018;**11**(5):1090–1096.

49 Ni L, Lu J. Interferon gamma in cancer immunotherapy. *Cancer Med*. 2018;**7**(9):4509–4516.

50 Karachaliou N, Gonzalez-Cao M, Crespo G, Drozdowskyj A, Aldeguer E, Gimenez-Capitan A, et al. Interferon gamma, an important marker of response to immune checkpoint blockade in non-small cell lung cancer and melanoma patients. *Ther Adv Med Oncol*. 2018;**10**:1758834017749748.

Genes	Name	logFC	P value
BDKRB2	bradykinin receptor B2	-1,339	2,419E-06
PLA2G16	phospholipase A2 group XVI	-1,010	2,947E-06
ITGB5	integrin subunit beta 5	-0,842	3,619E-06
S100A9	S100 calcium binding protein A9	-0,936	6,849E-06
WNT4	Wnt family member 4	-1,674	7,006E-06
C14orf132	chromosome 14 open reading frame 132	-1,006	1,020E-05
TIMP3	TIMP metallopeptidase inhibitor 3	-0,873	2,878E-05
MAT1A	methionine adenosyltransferase 1A	-1,170	4,665E-05
S100A7	S100 calcium binding protein A7	-1,658	6,605E-05
ACBD5	acyl-CoA binding domain containing 5	-0,836	7,813E-05
KALRN	kalirin RhoGEF kinase	-0,978	7,912E-05
OTOF	otoferlin	-1,668	8,393E-05
MAEA	macrophage erythroblast attacher	-0,706	1,398E-04
STC1	stanniocalcin 1	-1,405	1,400E-04
GRAMD2	GRAM domain containing 2A	-1,822	1,404E-04
KCNK5	potassium two pore domain channel subfamily K member 5	-1,075	1,550E-04

Genes	Name	logFC	P value
ARMT1	acidic residue methyltransferase 1	0,681	4,137E-04
SLC9B1	olute carrier family 9 member B1	1,567	6,278E-04
GCSH	glycine cleavage system protein H	1,216	1,296E-03
WDR93	WD repeat domain 93	1,495	1,429E-03
GALNTL6	polypeptide N-acetylgalactosaminyltransferase like 6	0,946	2,964E-03
ID1	inhibitor of DNA binding 1, HLH protein	0,650	4,329E-03
SAMD13	sterile alpha motif domain containing 13	1,194	5,618E-03
AARD	alanine and arginine rich domain containing protein	1,049	5,834E-03
DYRK4	dual specificity tyrosine phosphorylation regulated kinase 4	0,948	6,614E-03
MAPK10	mitogen-activated protein kinase 10	1,012	7,211E-03
KLB	klotho beta	0,805	8,566E-03
RPL39	ribosomal protein L39	0,839	8,795E-03
FKBP7	FK506 binding protein 7	1,027	9,174E-03

Table 1. Top genes down-regulated (upper panel) or up-regulated (lower panel) after RIP140 mRNA knock-down. Genes are listed from lower to higher p values.

Pathway	Gene ranks	NES	pval	padj
interferon−gamma−mediated signaling pathway // BP		−2.27	2.4e−05	7.0e−03
type I interferon signaling pathway // BP		−2.27	2.4e−05	7.0e−03
Interferon alpha/beta signaling // Reactome		−2.26	2.4e−05	7.0e−03
Interferon gamma signaling // Reactome		−2.21	2.4e−05	7.0e−03
Interferon Signaling // Reactome		−2.09	2.7e−05	7.0e−03
aromatase activity // MF		−2.09	2.1e−05	7.0e−03
T cell costimulation // BP		−2.07	7.0e−05	1.2e−02
establishment of skin barrier // BP		−2.03	1.9e−04	2.3e−02
positive regulation of Wnt signaling pathway // BP		−2.01	3.3e−04	3.4e−02
actomyosin structure organization // BP		−2.00	3.9e−04	3.6e−02
keratinization // BP		−2.00	3.8e−04	3.6e−02
chromatin DNA binding // MF		−1.99	1.8e−04	2.3e−02
PKMTs methylate histone lysines // Reactome		−1.94	3.9e−04	3.6e−02
Z disc // CC		−1.93	9.7e−05	1.6e−02
Keratinization // Reactome		−1.93	1.4e−04	1.9e−02
Extracellular matrix organization // Reactome		−1.93	2.8e−05	7.0e−03
Viral mRNA Translation // Reactome		1.92	5.1e−05	1.0e−02
cytokine−mediated signaling pathway // BP		−1.92	2.8e−05	7.0e−03
response to hypoxia // BP		−1.92	2.6e−05	7.0e−03
neuropeptide signaling pathway // BP		1.92	4.8e−04	4.2e−02
extracellular matrix // CC		−1.89	5.1e−05	1.0e−02

Table 2. Interferon signaling is a target of RIP140. Gene set enrichment analysis of RIP140 knockdown consequences under basal conditions combining GO Biological Process terms and Reactome pathways.

Figure Legends

Figure 1. Validation of RNA sequencing results. (A) MELN cells were transfected with either control siRNA (siCtl), or siRIP140. Total RNAs were subjected to RT-qPCR assays, and quantification of RIP140 mRNA was expressed relatively to the control condition (siCtl). (B) MELN cells were transfected as in A and then treated or not with estradiol (10^{-8} M). Luciferase mRNA was quantified and results expressed as above described. MCF7 cells were transfected with siCtl or siRIP140 (C) or with pEF-RIP140 or the empty vector (D). Quantification of mRNAs was done as described in (A). Statistical analyses were performed using the Mann-Whitney test. *p<0.05; **p<0.01; ***p<0.001.

Figure 2. RIP140 stimulates GBP1 expression. (A) MCF7, T47D and MDA-MB-231 cells were transfected with either siCtl or siRIP140. RNAs were subject to RT-qPCR assays, and quantification of GBP1 mRNA was expressed relatively to siCtl condition. (B) MCF7, T47D and MDA-MB-231 cells were transfected with pRL-CMV-renilla and pro3757-GBP1 plasmids together with siCtl or siRIP140. Luciferase values were normalized to the renilla luciferase control and expressed relatively to the siCtl condition. MCF7 (C) and T47D (D) were transfected with pRL-CMV-renilla and pro3757-GBP1 plasmids together with increasing amounts of RIP140 expressing plasmid. Luciferase values are expressed as above described. Statistical analyses were performed using the Mann-Whitney test. *p<0.05, **p<0.01; ***p<0.001.

Figure 3. RIP140 regulates GBP1 gene expression through ISRE. Schematic representation of pro237-GBP1 (A) and ΔISRE (B). MCF7, T47D and MDA-MB-231 cells were transfected with pRL-CMV-renilla and either pro237-GBP1 (C) or ΔISRE (D) plasmids, siCtl and siRIP140. Luciferase values were normalized to the renilla luciferase control and expressed relatively to the siCtl condition. (E) Left panel: schematic representation of pISRE-F-luc. Right panel: MCF7 and T47D cells were transfected with siCtl and siRIP140 together with pISRE-F-luc and pRL-CMV-renilla. Luciferase values were expressed as in (C and D). Statistical analyses were performed using the Mann-Whitney test. **p<0.01; ***p<0.001.

Figure 4. RIP140 decreases IFN-dependent GBP1 gene expression. (A) MCF7,

T47D and MDA-MB-231 cells were either treated with vehicle or IFNγ (10 µg/ml) during 24h. RNAs were subjected to RT-qPCR assays, and quantification of GBP1 mRNA was expressed relatively to siCtl condition. (B) MCF7 cells were transfected with either siCtl or siRIP140 and then treated with increasing doses of IFNγ. RNAs were subject to RT-qPCR assays, and quantification of GBP1 mRNA was expressed relatively to siCtl condition. (C) MCF7 cells were transfected with either siCtl or siRIP140 and treated with either vehicle or IFNγ (10 µg/ml) during 24h. Protein extracts were submitted to western-blotting using an anti-GBP1 antibody. Relative intensity of the bands is determined by the ratio between GBP1 specific and total protein bands. (D) MCF7, T47D and MDA-MB-231 cells were transfected with either siCtl or siRIP140. Cells were then treated as in (A). GBP1 was quantified by RT-qPCR and results are expressed as the ratio between IFNγ and vehicle treatment, relatively to siCtl condition. (E) MCF7, T47D and MDA-MB-231 cells were transfected with pRL-CMV-renilla and pro3757-GBP1 plasmids. MCF7 (F) and T47D (G) cells were transfected with increasing doses of pEF-RIP140, pRL-CMV-renilla and pro3757-GBP1 plasmids. Cells (E, F and G) were treated and results expressed as in (D). Statistical analyses were performed using the Mann-Whitney test. **$p<0.01$; ***$p<0.001$.

Figure 5. RIP140 and GBP1 regulate MCF7 and MDA-MB-231 cell proliferation. (A) MCF7 (left panel) and MDA-MB-231 (right panel) cells were treated with IFNγ (10 µg/ml) or vehicle. Cell proliferation was measured over 7 days. Absorbance of Formazan crystals was read on a spectrophotometer. (B) MCF7 (left panel) and MDA-MB-231 (right panel) cells were transfected with either siCtl or siRIP140. Cell proliferation was quantified as in (A). Cell proliferation was quantified as in (A). (C) MCF7 (left panel) and MDA-MB-231 (right panel) cells were transfected with siCtl or siRIP140. Cell proliferation was monitored as in (A) and results from day 6 were expressed relative to treatment with vehicle (DMSO). (D) MDA-MB-231 cells were transfected with either siCtl or siGBP1. Cell proliferation was quantified as in (A). (E) MDA-MB-231 cells were transfected with either siCtl, siRIP140, siGBP1 or a combination of siRIP140 and siGBP1. Cell proliferation was monitored as in (A) and results from day 6 were expressed relative to siCtl or siGBP1. Statistical analyses were performed using the Mann-Whitney test. **$p<0.01$; ***$p<0.001$.

Figure 6. IFNγ expression is good prognosis only when RIP140 is low. The Kaplan-Meier method was used to estimate overall survival of patients from the TCGA dataset. (A) The analysis was performed according to *IFNG* gene expression levels. (B) The same analysis was done on patients presenting low levels (left panel) or high levels (right panel) of *NRIP1* gene expression.

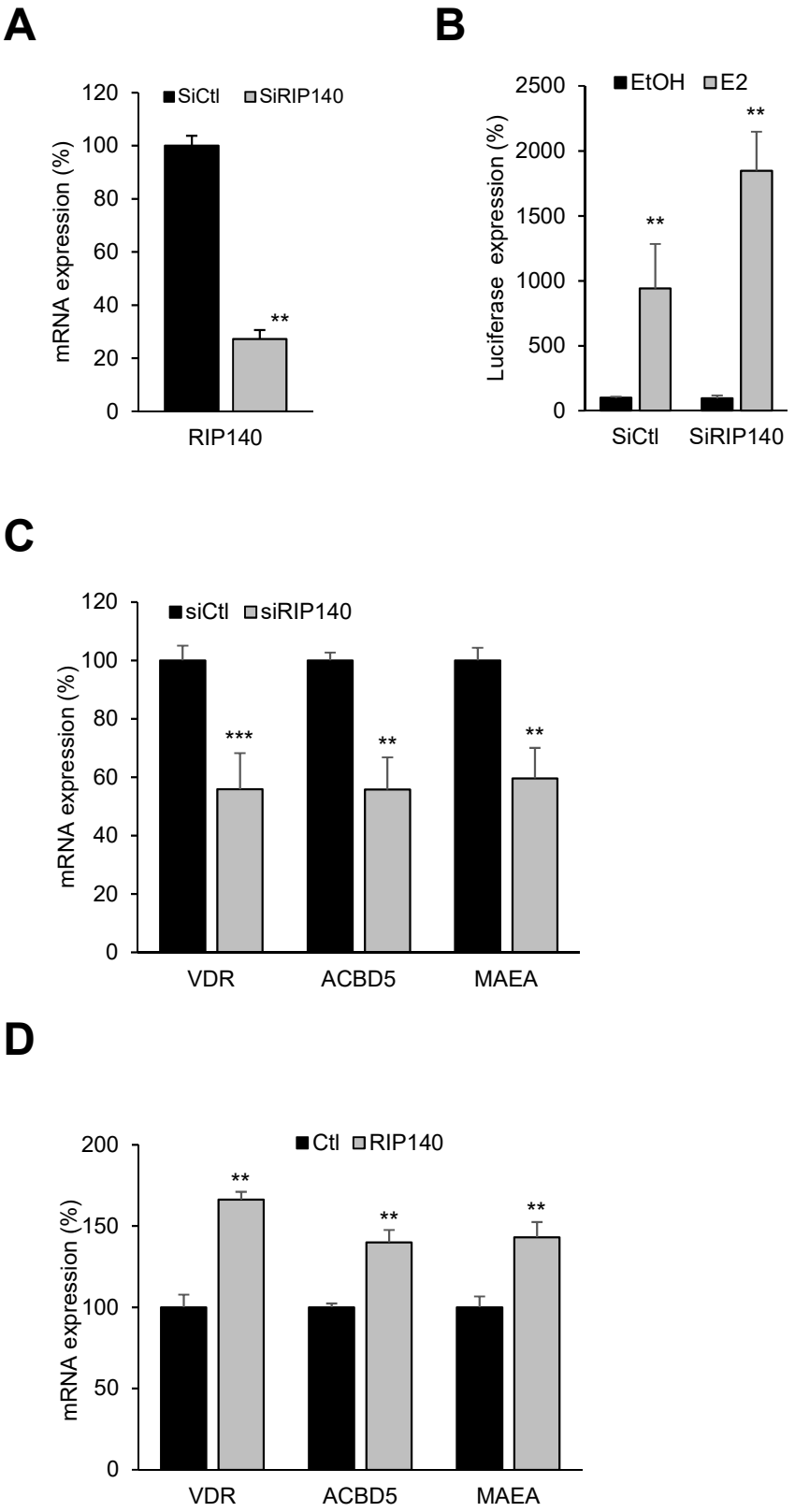
A
SiCtl
SiRIP140
mRNA expression (%)
120
100
80
60
40
20
0
**
RIP140
B
EtOH
E2
Luciferase expression (%)
2500
2000
1500
1000
500
0
**
**
SiCtl
SiRIP140
C
siCtl
siRIP140
mRNA expression (%)
120
100
80
60
40
20
0
***
**
**
VDR
ACBD5
MAEA
D
Ctl
RIP140
mRNA expression (%)
200
150
100
50
0
**
**
**
VDR
ACBD5
MAEA

Figure 1

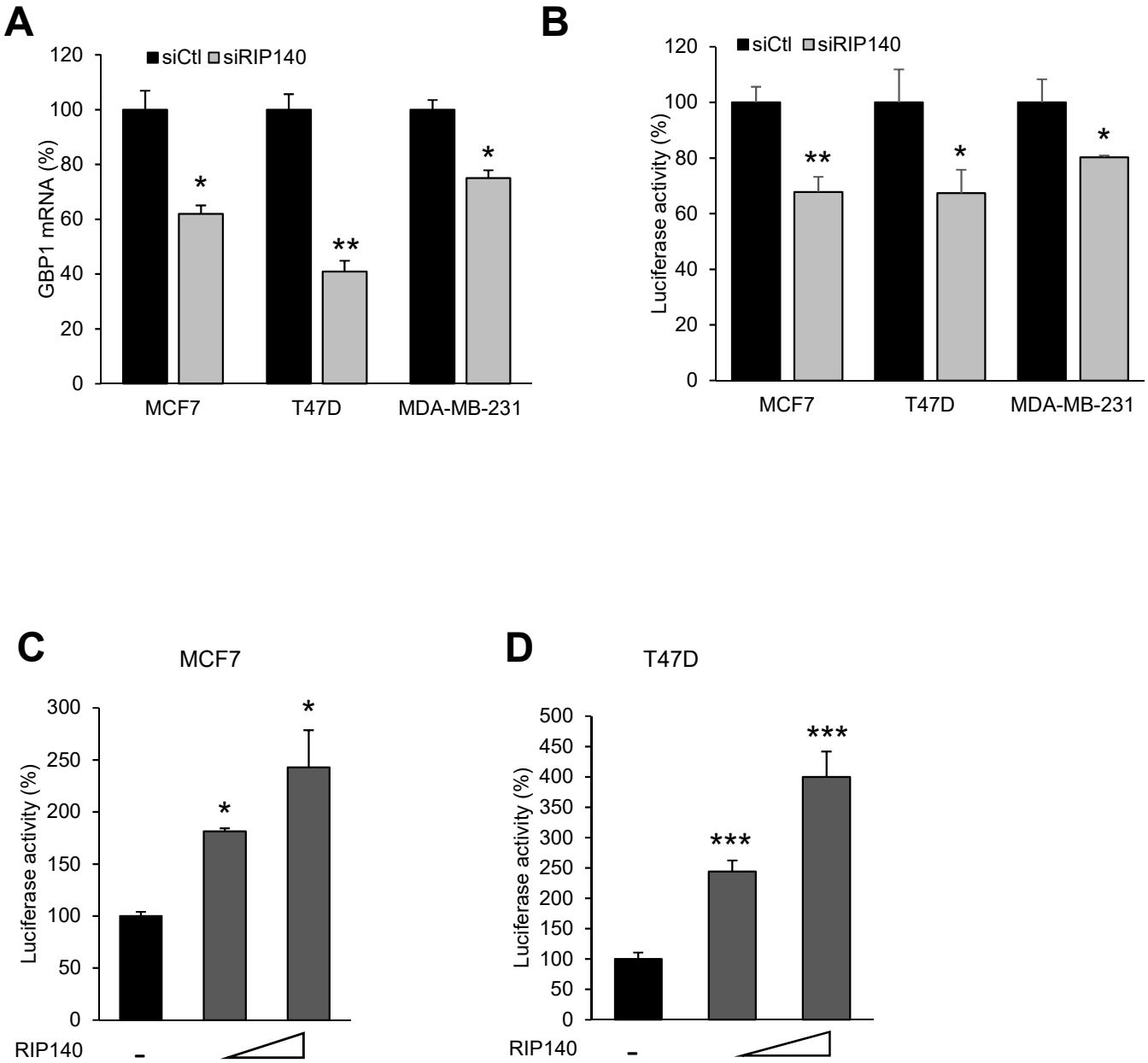
A
siCtl
siRIP140
GBP1 mRNA (%)
120
100
80
60
40
20
0
*
**
*
MCF7
T47D
MDA-MB-231
B
siCtl
siRIP140
Luciferase activity (%)
120
100
80
60
40
20
0
**
*
*
MCF7
T47D
MDA-MB-231
C
MCF7
Luciferase activity (%)
300
250
200
150
100
50
0
*
*
RIP140
-
D
T47D
Luciferase activity (%)
500
450
400
350
300
250
200
150
100
50
0
***
***
RIP140
-

Figure 2

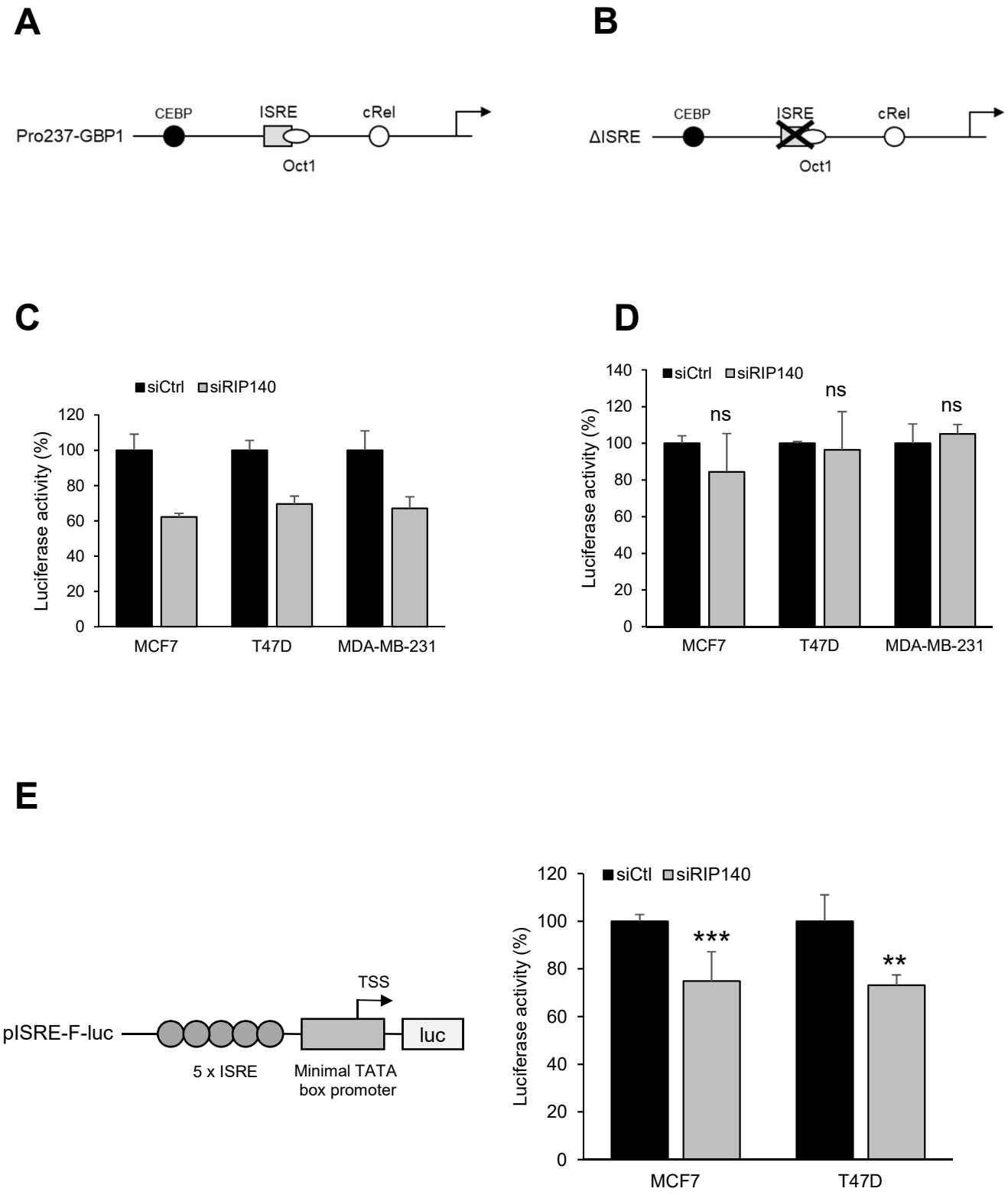
A
Pro237-GBP1
CEBP
ISRE
cRel
Oct1
B
ΔISRE
CEBP
ISRE
cRel
Oct1
C
siCtrl
siRIP140
Luciferase activity (%)
120
100
80
60
40
20
0
MCF7
T47D
MDA-MB-231
D
siCtrl
siRIP140
Luciferase activity (%)
140
120
100
80
60
40
20
0
ns
ns
ns
MCF7
T47D
MDA-MB-231
E
pISRE-F-luc
TSS
luc
5 x ISRE
Minimal TATA box promoter
siCtl
siRIP140
Luciferase activity (%)
120
100
80
60
40
20
0
***
**
MCF7
T47D

Figure 3

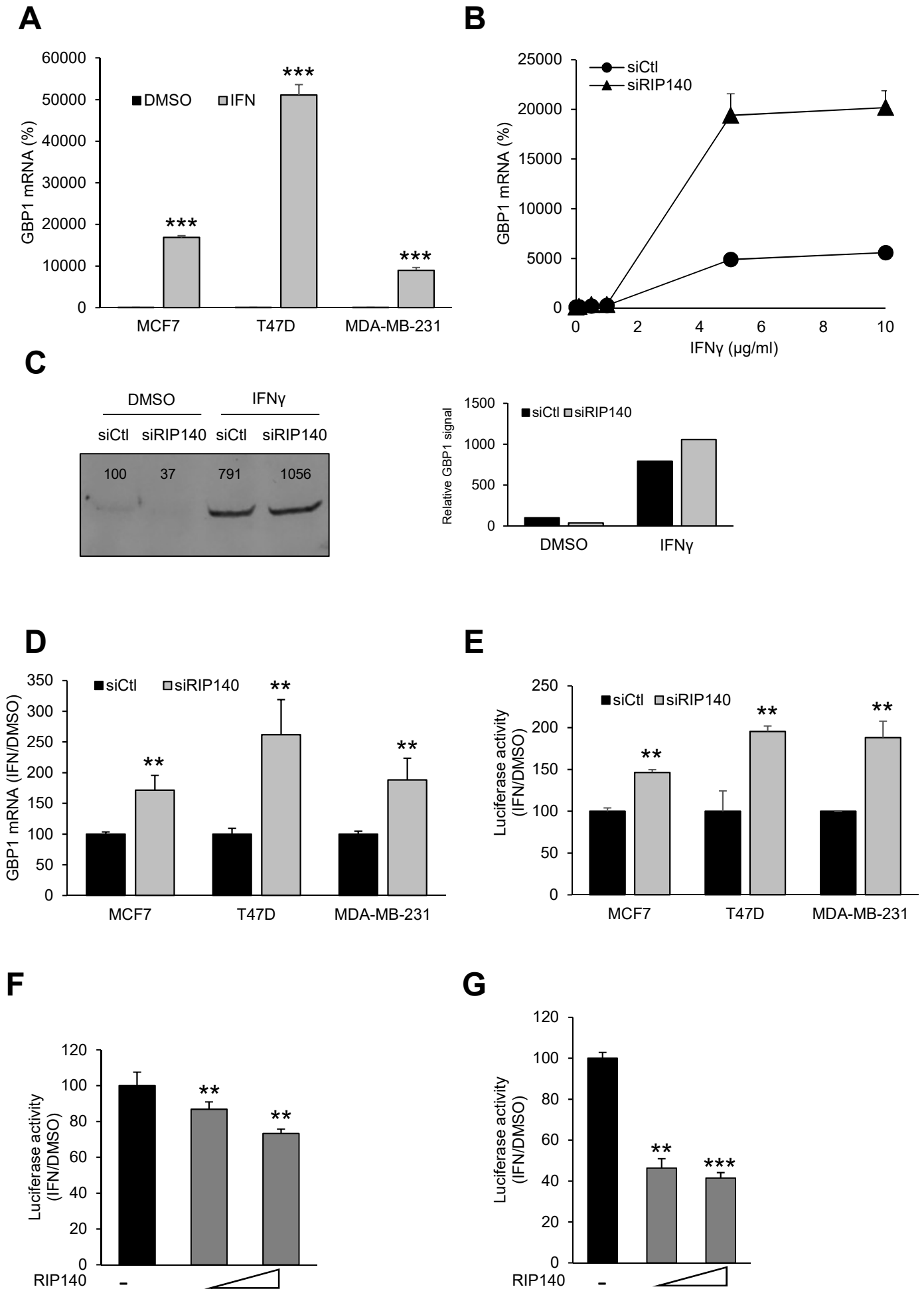
A
60000
50000
40000
30000
20000
10000
0
GBP1 mRNA (%)
DMSO
IFN
***
***
***
MCF7
T47D
MDA-MB-231
B
25000
20000
15000
10000
5000
0
GBP1 mRNA (%)
siCtl
siRIP140
0
2
4
6
8
10
IFNγ (μg/ml)
C
DMSO
IFNγ
siCtl
siRIP140
siCtl
siRIP140
100
37
791
1056
1500
1000
500
0
Relative GBP1 signal
siCtl
siRIP140
DMSO
IFNγ
D
350
300
250
200
150
100
50
0
GBP1 mRNA (IFN/DMSO)
siCtl
siRIP140
**
**
**
MCF7
T47D
MDA-MB-231
E
250
200
150
100
50
0
Luciferase activity (IFN/DMSO)
siCtl
siRIP140
**
**
**
MCF7
T47D
MDA-MB-231
F
120
100
80
60
40
20
0
Luciferase activity (IFN/DMSO)
**
**
RIP140
-
G
120
100
80
60
40
20
0
Luciferase activity (IFN/DMSO)
**
***
RIP140
-

Figure 4

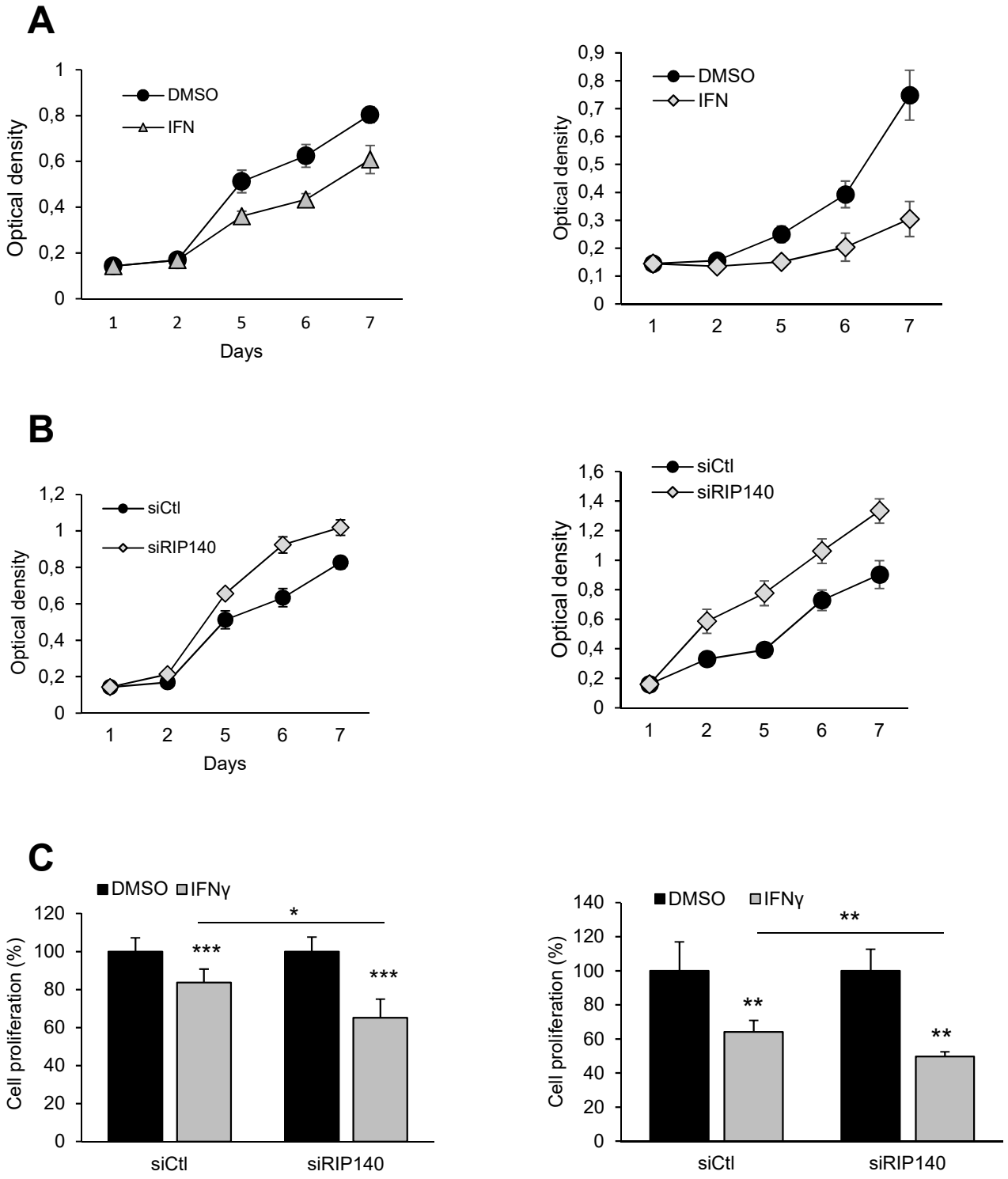
A
DMSO
IFN
Optical density
Days
B
siCtl
siRIP140
C
DMSO
IFNγ
Cell proliferation (%)
siCtl
siRIP140

Figure 5

A

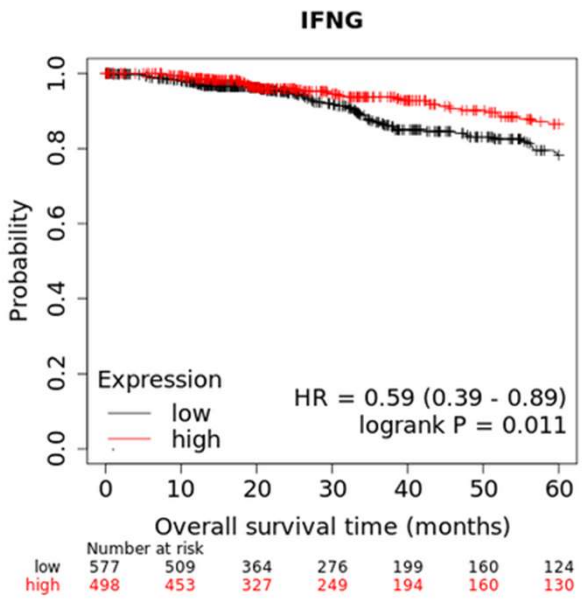
IFNG
Probability
1.0
0.8
0.6
0.4
0.2
0.0
Expression
low
high
HR = 0.59 (0.39 - 0.89)
logrank P = 0.011
0
10
20
30
40
50
60
Overall survival time (months)
Number at risk
low 577 509 364 276 199 160 124
high 498 453 327 249 194 160 130

B

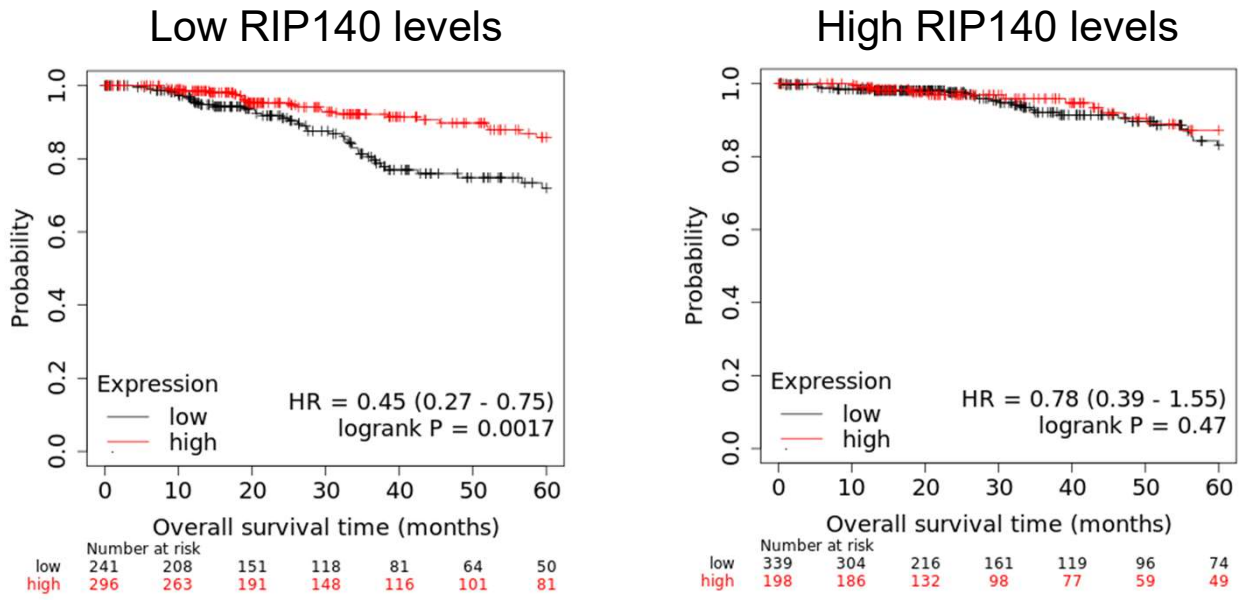
Low RIP140 levels
High RIP140 levels
Probability
1.0
0.8
0.6
0.4
0.2
0.0
Expression
low
high
HR = 0.45 (0.27 - 0.75)
logrank P = 0.0017
HR = 0.78 (0.39 - 1.55)
logrank P = 0.47
0
10
20
30
40
50
60
Overall survival time (months)
Number at risk
low 241 208 151 118 81 64 50
high 296 263 191 148 116 101 81
low 339 304 216 161 119 96 74
high 198 186 132 98 77 59 49

Figure 6